Supplementary Information

One F atom matters: synthesis, aggregation-induced emission and stimuli responsiveness of three isomers of fluoro/formyl substituted tetraphenylethene derivatives

Tianrui Li[a], Jinling Miao*[b], Chunyue Xu[a], Yong Nie*[a], Wei Liu[a], Yexin Li[b], Guangning Liu[b], Xuchuan Jiang*[a]

[a]Institute for Smart Materials & Engineering, University of Jinan, No. 336 Nanxinzhuang West Road, 250022 Jinan, P. R. China
[b]School of Chemistry and Chemical Engineering, Shandong Provincial Key Laboratory of Fluorine Chemistry and Chemical Materials, University of Jinan, No. 336 Nanxinzhuang West Road, 250022 Jinan, P. R. China

Contents

Experimental section

General

Standard Schlenk techniques were used for the synthetic reactions under Ar. The solvents were commercially available and used without further purification. IR spectra were recorded in the range 450-4000 cm^{-1} on a Perkin Elmer Tensor II spectrometer using KBr pellets. ^{1}H- and ^{13}C-NMR analyses were performed using a Bruker Avance III 600 MHz spectrometer. As internal references for ^{1}H- and ^{13}C-NMR spectroscopy the signals of $CDCl_3$ were used and calculated relative to tetramethylsilane (TMS). ^{19}F-NMR spectra were recorded in dichloromethane solutions (D_2O was added for locking) on a Bruker AVANCE III 500 spectrometer. Melting points were measured with a SGW X-4 apparatus and are not corrected. The high resolution mass spectra were measured with a Thermo Fisher Scientific LTQ FTICR-MS instrument (DART positive ion mode). UV-Vis spectra were recorded using a UV-9000S spectrometer. Emission spectra were measured with an Edinburgh FLS920 fluorimeter using a front-face solid sample configuration for solid samples. Absolute fluorescence quantum yields were obtained using an integrating sphere. For the variable temperature emission spectra of the powder samples, a temperature controller (TCB1402C) made by Techcomp company was applied, and for the silica gel composites on TLC plates, a hot plate was used to heat up the TLC plates and the emission spectra were then measured as soon as possible. The dynamic light scattering measurements were conducted on a Malvern Zetasizer Nano ZS.

Synthesis of compound 1

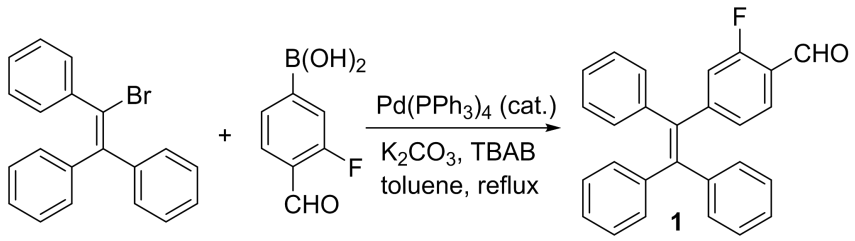

Under argon, triphenylvinylbromide (670.14 mg, 2.00 mmol), tetrabutylammonium bromide (89 mg, 0.27 mmol), 3-fluoro-4-formylphenyl boronic acid (403.2 mg, 2.40 mmol), anhydrous K_2CO_3 (830.2 mg, 6.00 mmol), $Pd(PPh_3)_4$ (106.0 mg, 0.092 mmol) and 20 mL of toluene and 5 mL of water were added to a Schlenk tube. The reaction mixture was stirred under reflux (oil bath 120 ^{o}C) for 6 h. A small amount of CH_2Cl_2 was added and the mixture was filtered, from the filtrate the organic phase was separated, and the water phase was extracted with CH_2Cl_2 (20 mL × 2). The organic phases were combined and dried with anhydrous Na_2SO_4 and separated using column chromatography (eluent

CH_2Cl_2/hexane = 1/1, *V*/*V*) to obtain a yellow greenish solid (compound **1**).

1: 692 mg, yield 91.5%; m.p.183.1-183.9 °C; R_f = 0.52 (eluent CH_2Cl_2/hexane = 1/1, *V*/*V*); IR (KBr, ν/cm^{-1}): 3071, 3051, 2854, 2760, 1690 (C=O), 1612, 1557, 1490, 1442, 1261 (C-F); ^{1}H NMR (600 MHz, $CDCl_3$) δ 10.23 (s, 1H), 7.58 (t, *J* = 7.7 Hz, 1H), 7.19 – 7.08 (m, 10H), 7.07 – 6.96 (m, 7H), 6.92 (d, *J* = 12 Hz, 1H), 6.82 (dd, *J* = 11.6, 1.6 Hz, 1H); ^{13}C NMR (151 MHz, $CDCl_3$) δ 187.03 (d, *J* = 5.03 Hz), 165.26, 163.55, 153.24, 153.18, 144.06, 142.82, 142.73, 142.45, 138.85 (d, *J* = 1.34 Hz), 131.35, 131.31, 131.27, 128.23 (d, *J* = 5.03 Hz), 127.96, 127.95, 127.92, 127.88, 127.87, 127.57, 127.25, 122.20, 122.14, 119.18, 119.04; ^{19}F NMR (377 MHz, CH_2Cl_2) δ -123.52; DART-MS *m/z* (%): calcd. for $C_{27}H_{19}FO$, 379.1493 $[M+H]^+$, found 379.1487.

Synthesis of compound 2

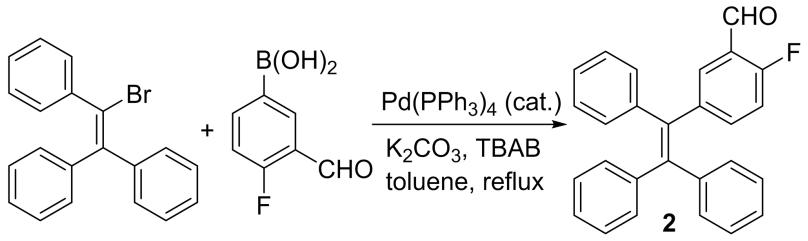

Under argon, triphenylvinylbromide (672.7 mg, 2.0 mmol), tetrabutylammonium bromide (92.1 mg, 0.28 mmol), 4-fluoro-3-formylphenyl boronic acid (407.8 mg, 2.40 mmol), anhydrous K_2CO_3 (831.7 mg，6.0 mmol), $Pd(PPh_3)_4$ (102 mg, 0.088 mmol) and 20 mLof toluene and 5 mL of waterwere added to a Schlenk tube. The reaction mixture was stirred under reflux (oil bath 120 °C) for 16 h. A small amount of CH_2Cl_2 was added and the mixture was filtered, from the filtrate the organic phase was separated, and the water phase was extracted with CH_2Cl_2 (20 mL × 2). The organic phases were combined and dried with anhydrous Na_2SO_4 and separated using column chromatography (eluent CH_2Cl_2/hexane = 1/1, *V*/*V*) to obtain a white solid (compound **2**).

2: 722 mg, yield 95.5%; m.p.157.6-158.1 °C; R_f= 0.33 (eluent CH_2Cl_2/hexane = 1/1, *V*/*V*); IR (KBr, ν/cm^{-1}): 3073, 3020, 2860, 2763, 1693 (C=O), 1599, 1489, 1258 (C-F); ^{1}H NMR (600 MHz, $CDCl_3$) δ 10.19 (s, 1H), 7.52 (dd, *J* = 6.7, 2.4 Hz, 1H), 7.15 – 7.08 (m, 10H), 7.04 – 6.97 (m, 6H), 6.89 (dd, *J* = 10.1, 8.6 Hz, 1H); ^{13}C NMR (151 MHz, $CDCl_3$) δ 187.30 (d, *J* = 6.10 Hz), 164.02, 162.30, 143.10, 143.06, 142.72, 142.66, 140.80 (d, *J* = 4.04 Hz), 139.30, 139.24, 138.69, 131.62, 131.38, 131.30, 131.26, 128.13, 127.90, 127.07 (d, *J* = 4.45 Hz), 126.94, 123.73, 123.68, 116.11, 115.97; ^{19}F NMR (377 MHz, CH_2Cl_2) δ -124.92; DART-MS *m/z* (%): calcd. for $C_{27}H_{19}FO$, 379.1493 $[M+H]^+$, found 379.1487.

Synthesis of compound 3

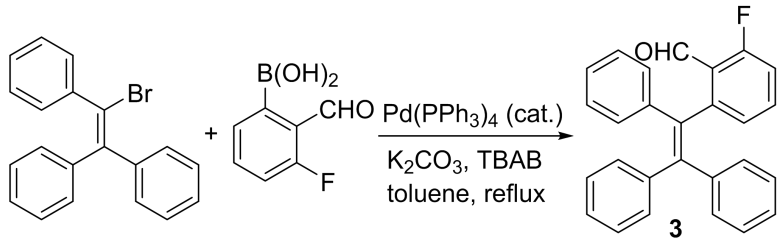

Under argon, triphenylvinylbromide (671.2 mg, 2.0 mmol), tetrabutylammonium bromide (79.8 mg, 0.25 mmol), 3-fluoro-2-formylphenyl boronic acid (403.6 mg, 2.40 mmol), anhydrous K_2CO_3 (830.3 mg, 6.0 mmol), $Pd(PPh_3)_4$ (108.8 mg, 0.094 mmol) and 20 mL of toluene and 5 mL of water were added to a Schlenk tube. The reaction mixture was stirred under reflux (oil bath 120 ^oC) for 16 h. A small amount of CH_2Cl_2 was added and the mixture was filtered, from the filtrate the organic phase was separated, and the water phase was extracted with CH_2Cl_2 (20 mL × 2). The organic phases were combined and dried with anhydrous Na_2SO_4 and separated using column chromatography (eluent CH_2Cl_2/hexane = 1/1, *V*/*V*) to obtain a light yellow solid (compound **3**).

3: 638.2 mg, yield 84 %; m.p. 105.7-106.3 ^oC; R_f = 0.31 (eluent CH_2Cl_2/hexane = 1/1, *V*/*V*); IR (KBr, ν/cm^{-1}): 3071, 3051, 2854, 2767, 1699 (C=O), 1603, 1568, 1490, 1465, 1240 (C-F); ^1H NMR (600 MHz, $CDCl_3$) δ 10.25 (s, 1H), 7.35 (td, *J* = 8.0, 5.4 Hz, 1H), 7.14 (t, *J* = 3.42 Hz, 4H), 7.08 (m, 9H), 7.03 – 6.98 (m, 4H), 6.95 (m, 3H); ^{13}C NMR (151 MHz, $CDCl_3$) δ 188.50 (d, *J* = 4.60 Hz), 164.61, 162.89, 147.77, 143.25, 142.83, 142.52, 141.87, 137.07, 134.46, 134.39, 131.27, 130.98, 130.70, 128.95 (d, *J*=3.29 Hz), 127.98, 127.88, 127.17 (d, *J* = 3.87 Hz), 126.98, 123.73, 123.68, 115.26, 115.12; ^{19}F NMR (377 MHz, CH_2Cl_2) δ -118.94; DART-MS *m/z* (%): calcd. for $C_{27}H_{19}FO$, 379.1493 $[M+H]^+$, found 379.1486.

Synthesis of compound TPE-2CHO

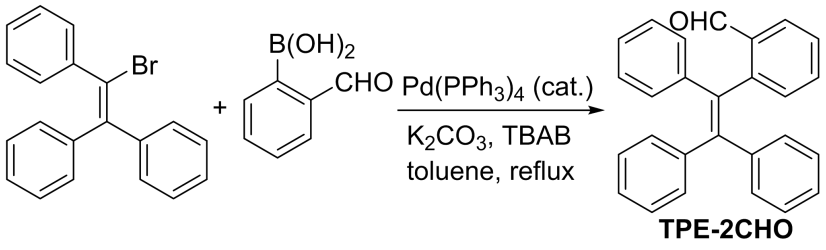

Under argon, triphenylvinylbromide (671.7 mg, 2.0 mmol), tetrabutylammonium bromide (66.7 mg, 0.2 mmol), 2-formylphenyl boronic acid (329.9 mg, 2.20 mmol), anhydrous K_2CO_3 (832.3 mg, 6.0 mmol), $Pd(PPh_3)_4$ (115.8 mg, 0.1 mmol), and 20 mL of toluene and 5 mL of water were added to a

Schlenk tube. The reaction mixture was stirred under reflux (oil bath 120 ºC) for 12 h. A small amount of CH_2Cl_2 was added and the reaction mixture was filtered, from the filtrate the organic phase was separated, and the water phase was extracted with CH_2Cl_2 (20 mL × 2). The organic phases were combined and dried with anhydrous Na_2SO_4 and separated using column chromatography (eluent CH_2Cl_2/hexane = 1/1, *V*/*V*) to obtain a light yellow solid (compound **TPE-2CHO**).

TPE-2CHO: 615.2 mg, yield 85 %; m.p. 95.7-96.0 ºC; R_f = 0.41 (eluent CH_2Cl_2/hexane = 1/1, *V*/*V*); IR (KBr, ν/cm^{-1}): 3051, 3024, 2833, 2739, 1693 (C=O), 1593, 1441, 754, 700; ^{1}H NMR (600 MHz, $CDCl_3$) δ 10.33 (s, 1H), 7.73 (m, 1H), 7.42 (td, *J* = 6.3, 7.6 Hz, 1H), 7.27 (t, *J* = 8.06 Hz, 1H), 7.21(d, *J* = 3.42 Hz, 4H), 7.20, 7.16 - 7.15 (m, 3H), 7.10 - 7.07 (m, 5H), 7.04 - 7.03 (m, 3H), 7.01 - 7.00 (m, 2H), 6.93 - 6.91(m, 2H); ^{13}C NMR (151 MHz, $CDCl_3$) δ 191.73 (d, *J* = 3.04 Hz), 147.16, 144.55, 142.69, 142.51, 142.47, 136.31, 134.13, 133.49, 132.66, 131.14, 130.89, 130.82, 127.97, 127.95, 127.85, 127.64, 127.44, 127.12, 126.99, 126.90; EI-MS *m/z* (%): calcd. for $C_{27}H_{21}O$, 361.46 $[M+H]^+$, found 361.40 (100%).

Table S1 Crystal data and structure refinement for **2**

Empirical formula	$C_{27}H_{19}FO$
Formula weight	378.42
Temperature/K	293(2)
Crystal system	monoclinic
Space group	$P2_1$
a/Å	10.2779(7)
b/Å	9.1125(5)
c/Å	11.3260(6)
α/°	90
β/°	106.418(7)
γ/°	90
Volume/Å^3	1017.51(11)
Z	2
ρ_{calc}g/cm^3	1.235
μ/mm^{-1}	0.08
F(000)	396
Crystal size/mm^3	0.1 × 0.1× 0.1

Radiation	Mo Kα (λ = 0.71073)
2Θ range for data collection/°	6.51 to 50.698
Index ranges	$-12 \le h \le 12$, $-10 \le k \le 10$, $-13 \le l \le 13$
Reflections collected	6090
Independent reflections	3498 [R_{int} = 0.0276, R_{sigma} = 0.0535]
Data/restraints/parameters	3498/1/262
Goodness-of-fit on F^2	0.97
Final R indexes [I>=2σ (I)]	R_1 = 0.0485, wR_2 = 0.1093
Final R indexes [all data]	R_1 = 0.0836, wR_2 = 0.1258
Largest diff. peak/hole / e $Å^{-3}$	0.27/-0.18
Flack parameter	-0.1(7)
CCDC deposition number	2100022

Table S2 Crystal data for **3**

Empirical formula	$C_{27}H_{19}FO$
Formula weight	378.42
Temperature/K	293(2)
Crystal system	monoclinic
Space group	$P2_1/n$
a/Å	12.0247(7)
b/Å	9.3443(5)
c/Å	21.2636(16)
α/°	90
β/°	93.711(6)
γ/°	90
Volume/$Å^3$	2384.2(3)
Z	4
ρ_{calc}g/cm^3	1.053
μ/mm^{-1}	0.07
F(000)	1096
Crystal size/mm^3	0.25 × 0.15× 0.1
Radiation	Mo Kα (λ = 0.71073)

Table S3 Selected bond lengths (Å)and torsion angles (°) for **2** and **3**.

	2	**3**
bond lengths	C8-C15 1.355 C3-F2 1.361 C6-C8 (F-Ar) 1.478 C8-C9 (Ph) 1.488 C15-C16 (Ph) 1.486 C15-C22 (Ph) 1.488	C8-C15 1.347 C3-F1 1.355 C7-C8 (F-Ar) 1.502 C8-C9 (Ph) 1.507 C15-C16 (Ph) 1.496 C15-C22 (Ph) 1.497
Selected torsion angles	C15-C8-C6-C5 (C=C-(F-Ar)) 42.86 C15-C8-C9-C14 (C=C-Ph) 50.855 C8-C15-C16-C17 (C=C-Ph) 47.566 C8-C15-C22-C27 (C=C-Ph) 48.295	C15-C8-C7-C6 (C=C-(F-Ar)) -69.81 C15-C8-C9-C14 (C=C-Ph) -51.44 C8-C15-C16-C17 (C=C-Ph) -46.76 C8-C15-C22-C27 (C=C-Ph) -51.61

Table S4 Diagrams of the frontier MOs of **1-3** and their non-fluorinated analogs [a]

Compounds	Frontier orbitals and energy gap
1	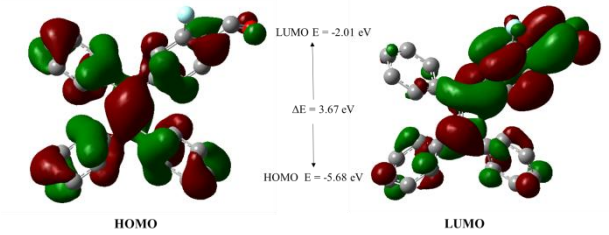
TPE-4CHO	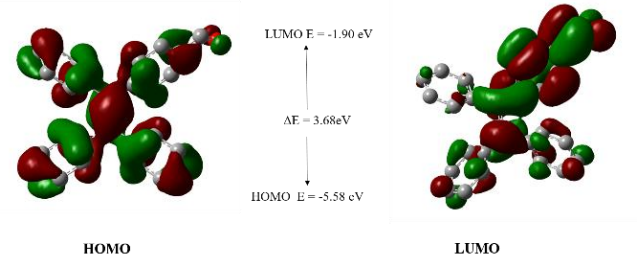
2	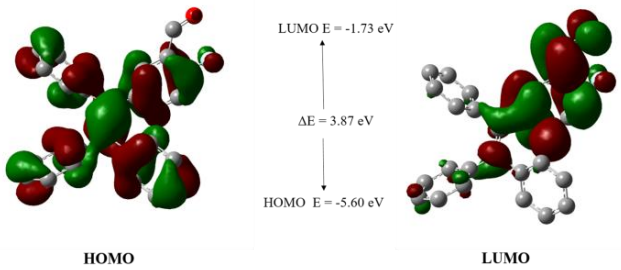
TPE-3CHO	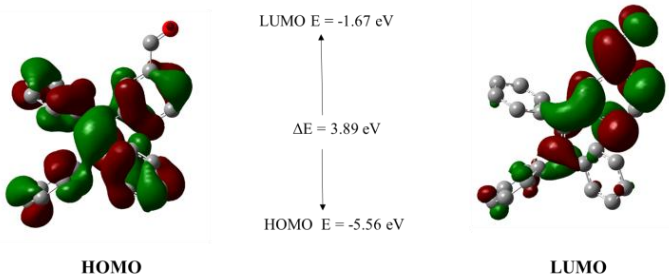

3	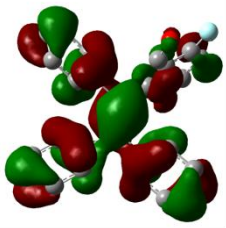	LUMO E = -1.86 eV ΔE = 3.84 eV HOMO E = -5.70 eV	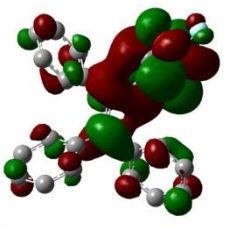	
	HOMO		**LUMO**	
TPE-2CHO	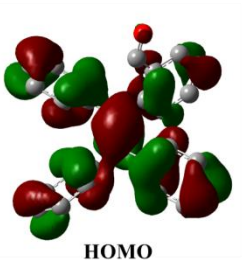	LUMO E = -1.77 eV ΔE = 3.84 eV HOMO E = -5.61 eV	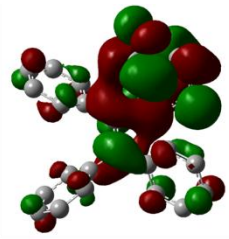	
	HOMO		**LUMO**	

[a] calculated at the B3LYP/6-31G (d, p) level of theory.

Table S5 Energy level of the HOMO/LUMO and HOMO-LUMO energy gap of **1-3** and their non-fluorinated analogs [a]

Compounds	E_{HOMO} (eV)	E_{LUMO} (eV)	ΔE (eV)
1	-5.86	-2.01	3.67
TPE-4CHO	-5.58	-1.90	3.68
2	-5.60	-1.73	3.87
TPE-3CHO	-5.56	-1.67	3.89
3	-5.70	-1.86	3.84
TPE-2CHO	-5.61	-1.77	3.84

[a] calculated at the B3LYP/6-31G (d, p) level of theory.

Table S6 Computed excitation energies and oscillator strengths for **1** from TD-DFT calculations in THF [a]

state	E (eV)	λ (nm)	*f*	transitions
1	3.1033	399.52	0.3769	HOMO→LUMO (99.3%)
2	3.6155	342.92	0.0002	HOMO - 5→LUMO (75.4%)
				HOMO - 5→LUMO + 1 (6.6%)
				HOMO - 4→LUMO (11.1%)
3	3.9988	310.05	0.2587	HOMO→LUMO +1 (95.7%)
4	4.0434	306.63	0.0337	HOMO - 3→LUMO (6.4%)
				HOMO - 2→LUMO (3.4%)
				HOMO - 1→LUMO (83.3%)
5	4.0434	306.63	0.0337	HOMO - 3→LUMO (6.5%)
				HOMO - 2→LUMO (3.5%)

				HOMO - 1→LUMO (83.2%)
6	4.1557	298.34	0.0046	HOMO - 3→LUMO (82.0%)
				HOMO - 2→LUMO (7.8%)
				HOMO - 1→LUMO (5.0%)
7	4.3635	284.14	0.0140	HOMO - 7→LUMO (8.1%)
				HOMO - 6→LUMO (13.4%)
				HOMO - 5→LUMO (7.1%)
				HOMO - 4→LUMO (52.6%)
				HOMO - 3→LUMO (2.2%)
				HOMO→LUMO + 2 (6.1%)
				HOMO→LUMO + 4 (2.6%)
8	4.3975	281.94	0.0285	HOMO - 7→LUMO (6.8%)
				HOMO - 6→LUMO (32.6%)
				HOMO - 5→LUMO (4.0%)
				HOMO - 4→LUMO (25.3%)
				HOMO→LUMO + 2 (26.6%)
9	4.5014	275.44	0.1000	HOMO - 7→LUMO (40.9%)
				HOMO - 6→LUMO (37.5%)
				HOMO→LUMO +2 (9.1%)
				HOMO→LUMO +3 (7.1%)
10	4.5977	269.67	0.1660	HOMO - 7→LUMO (33.3%)
				HOMO - 6→LUMO (6.5%)
				HOMO - 4→LUMO (2.2%)
				HOMO→LUMO +2 (48.5%)

[a] calculated at the B3LYP/6-31G (d, p) level of theory.

Table S7 Computed excitation energies and oscillator strengths for **2** from TD-DFT calculations in THF [a]

state	E (eV)	λ (nm)	*f*	transitions
1	3.1996	387.50	0.0322	HOMO→LUMO (98.5%)
2	3.6508	339.61	0.4705	HOMO→LUMO +1 (97.3%)
3	3.6859	336.38	0.0087	HOMO - 6→LUMO (3.7%)
				HOMO - 5→LUMO (54.9%)
				HOMO - 4→LUMO (33.3%)
4	4.3424	285.52	0.0185	HOMO - 2→LUMO (12.8%)
				HOMO - 1→LUMO +1 (80.2%)
5	4.3859	282.69	0.0308	HOMO - 3→LUMO (2.4%)
				HOMO - 2→LUMO (11.8%)
				HOMO - 1→LUMO + 1 (6.8%)
				HOMO - 1→LUMO + 1 (6.8%)
				HOMO→LUMO + 2 (64.8%)
6	4.4346	279.58	0.0151	HOMO - 3→LUMO (4.7%)
				HOMO - 2→LUMO (65.9%)
				HOMO - 2→LUMO + 1 (2.7%)

				HOMO - 1→LUMO + 1 (6.3%)
				HOMO - 1→LUMO + 2 (14.9%)
7	4.5095	274.94	0.0432	HOMO - 3→LUMO (80.4%)
				HOMO - 1→LUMO +1 (3.5%)
				HOMO→LUMO +2 (8.9%)
8	4.5656	271.56	0.0379	HOMO - 6→LUMO (3.2%)
				HOMO - 4→LUMO (3.3%)
				HOMO - 4→LUMO + 1 (2.2%)
				HOMO - 3→LUMO (6.1%)
				HOMO - 3→LUMO + 1 (4.7%)
				HOMO - 1→LUMO + 1(10.3%)
				HOMO→LUMO + 3 (61.0%)
9	4.5826	270.55	0.0403	HOMO - 3→LUMO (2.0%)
				HOMO - 1→LUMO (2.1%)
				HOMO - 1→LUMO + 1 (59.8%)
				HOMO→LUMO + 2 (2.7%)
				HOMO→LUMO + 3 (12.0%)
				HOMO→LUMO + 4 (11.4%)
				HOMO→LUMO + 5 (2.5%)
10	4.6246	268.10	0.0757	HOMO - 7→LUMO (15.5%)
				HOMO - 6→LUMO (7.6%)
				HOMO - 5→LUMO (10.0%)
				HOMO - 4→LUMO (23.5%)
				HOMO - 2→LUMO + 1 (12.6%)
				HOMO→LUMO + 3 (11.4%)
				HOMO→LUMO + 4 (4.6%)
				HOMO→LUMO + 6 (2.0%)

[a] calculated at the B3LYP/6-31G (d, p) level of theory.

Table S8 Computed excitation energies and oscillator strengths for **3** from TD-DFT calculations in THF [a]

state	E (eV)	λ (nm)	*f*	transitions
1	3.0910	401.11	0.1101	HOMO→LUMO (97.2%)
2	3.4807	356.21	0.0048	HOMO - 7→LUMO (3.9%)
				HOMO - 6→LUMO (2.1%)
				HOMO - 4→LUMO (51.9%)
				HOMO - 4→LUMO + 1 (3.5%)
				HOMO - 2→LUMO (6.0%)
				HOMO - 1→LUMO (25.0%)
3	3.9234	316.01	0.3431	HOMO→LUMO +1 (96.8%)
4	4.1228	300.73	0.0459	HOMO - 6→LUMO (2.3%)
				HOMO - 4→LUMO (7.9%)
				HOMO - 2→LUMO (23.7%)
				HOMO - 1→LUMO (59.8%)

5	4.2380	292.55	0.0199	HOMO - 3→LUMO (89.7%)
				HOMO - 2→LUMO (3.5%)
				HOMO→LUMO +2 (2.5%)
6	4.2400	292.42	0.0002	HOMO - 5→LUMO (2.5%)
				HOMO - 4→LUMO (18.2%)
				HOMO - 3→LUMO (3.1%)
				HOMO - 2→LUMO (62.1%)
				HOMO - 1→LUMO (9.8%)
7	4.3995	281.82	0.0149	HOMO - 6→LUMO (21.2%)
				HOMO - 5→LUMO (21.0%)
				HOMO - 4→LUMO (4.0%)
				HOMO→LUMO + 2(44.9%)
8	4.4923	275.99	0.0031	HOMO - 6→LUMO (19.8%)
				HOMO - 5→LUMO (61.7%)
				HOMO→LUMO + 2 (6.3%)
				HOMO→LUMO + 3 (6.2%)
9	4.5631	271.71	0.2944	HOMO - 8→LUMO (2.1%)
				HOMO - 6→LUMO (45.6%)
				HOMO - 5→LUMO (3.4%)
				HOMO - 4→LUMO (2.3%)
				HOMO→LUMO +2 (48.5%)
10	4.6529	266.46	0.0032	HOMO - 8→LUMO (3.7%)
				HOMO - 7→LUMO (73.7%)
				HOMO - 4→LUMO (5.0%)
				HOMO - 4→LUMO + 1 (3.7%)
				HOMO - 1→LUMO +1 (3.0%)
				HOMO→LUMO +4 (4.5%)

[a] calculated at the B3LYP/6-31G (d, p) level of theory.

Reference for the Gaussian package for the DFT calculations:

M. J. Frisch, G. W. Trucks, H. B. Schlegel, G. E. Scuseria, M. A. Robb, J. R. Cheeseman, G. Scalmani, V. Barone, B. Mennucci, G. A. Petersson, H. Nakatsuji, M. Caricato, X. Li, H. P. Hratchian, A. F. Izmaylov, J. Bloino, G. Zheng, J. L. Sonnenberg, M. Hada, M. Ehara, K. Toyota, R. Fukuda, J. Hasegawa, M. Ishida, T. Nakajima, Y. Honda, O. Kitao, H. Nakai, T. Vreven, J. A. Montgomery, Jr., J. E. Peralta, F. Ogliaro, M. Bearpark, J. J. Heyd, E. Brothers, K. N. Kudin, V. N. Staroverov, R. Kobayashi, J. Normand, K. Raghavachari, A. Rendell, J. C. Burant, S. S. Iyengar, J. Tomasi, M. Cossi, N. Rega, J. M. Millam, M. Klene, J. E. Knox, J. B. Cross, V. Bakken, C. Adamo, J. Jaramillo, R. Gomperts, R. E. Stratmann, O. Yazyev, A. J. Austin, R. Cammi, C. Pomelli, J. W. Ochterski, R. L. Martin, K. Morokuma, V. G. Zakrzewski, G. A. Voth, P. Salvador, J. J. Dannenberg, S. Dapprich, A. D. Daniels, O. Farkas, J. B. Foresman, J. V. Ortiz, J. Cioslowski, and D. J. Fox, Gaussian 09, Revision A.02, Gaussian, Inc., Wallingford CT, 2009.

Table S9 Emission lifetime data of solid samples of **1-3**

Compounds	τ_1 (ns)	percent	τ_2 (ns)	percent	τ (ns)
1	0.4682	86.05	2.0303	13.95	0.69
2	0.5165	41.64	1.0344	58.36	0.82
3	0.2819	91.72	0.4686	8.28	0.38

Table S10 Photophysical data for **1**, **TPE-4CHO**, **2**and **TPE-3CHO** at different temperatures

Compounds	λ_{em} [a](nm)					
	r. t.	70 ℃	100 ℃	120 ℃	140 ℃	cooling to r. t.
1	482	477	474	471	470	481
2	460	452	451	450	448	458
TPE-3CHO	462	460	458	458	458	458
TPE-4CHO	486	486	486	-	486	486

[a] λ_{ex} = 380 nm

Table S11 Photophysical data for the silica gel composites with **1**, **TPE-4CHO** and **2** at different temperatures

Composite	λ_{em} [a](nm)				
	r. t.	70 ℃	100 ℃	120 ℃	140 ℃
1	521	516	510	503	498
2	496	501	502	501	501
TPE-4CHO	512	510	512	511	511

[a] λ_{ex} = 380 nm

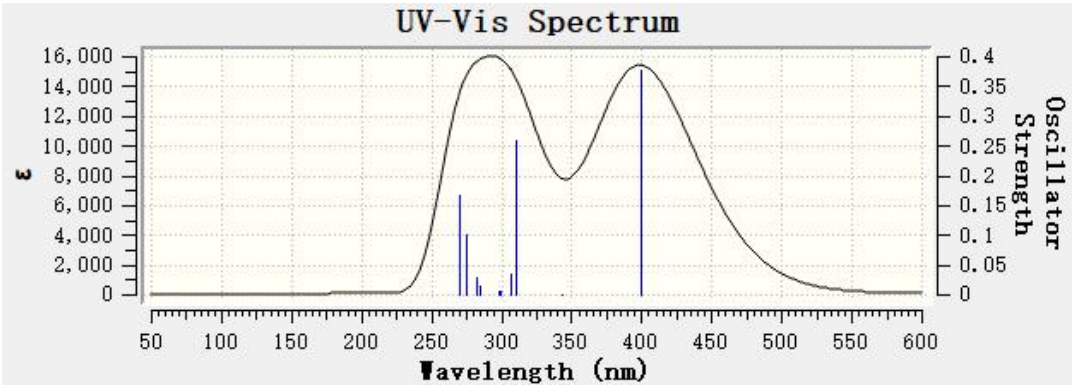

Fig. S1 Absorption spectrum of **1** in THF by DFT calculation

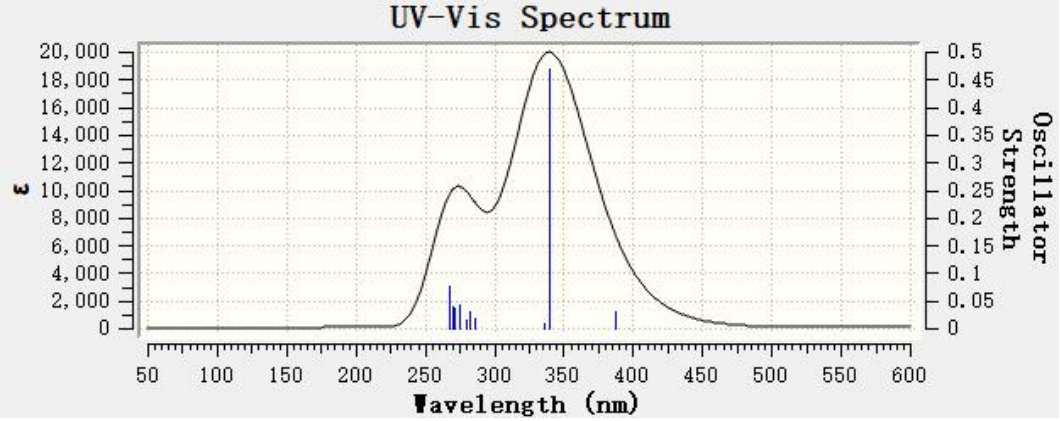

Fig. S2 Absorption spectrum of **2** in THF by DFT calculation

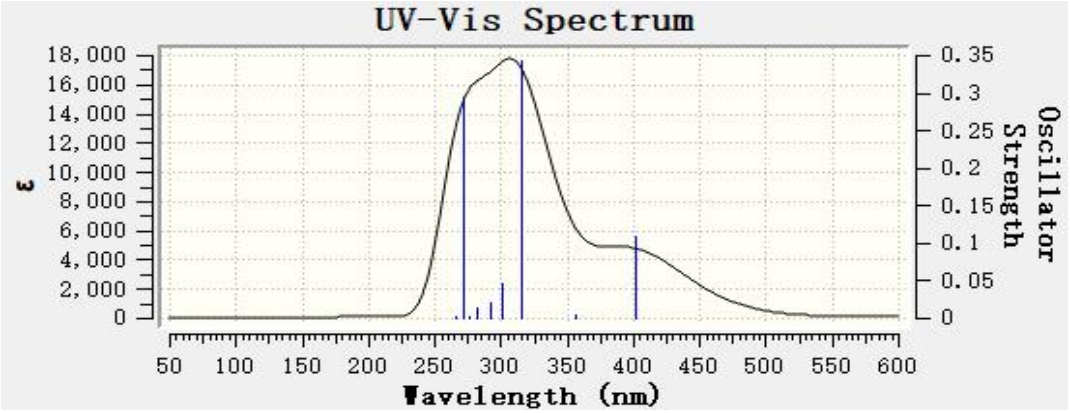

Fig. S3 Absorption spectrum of **3** in THF by DFT calculation

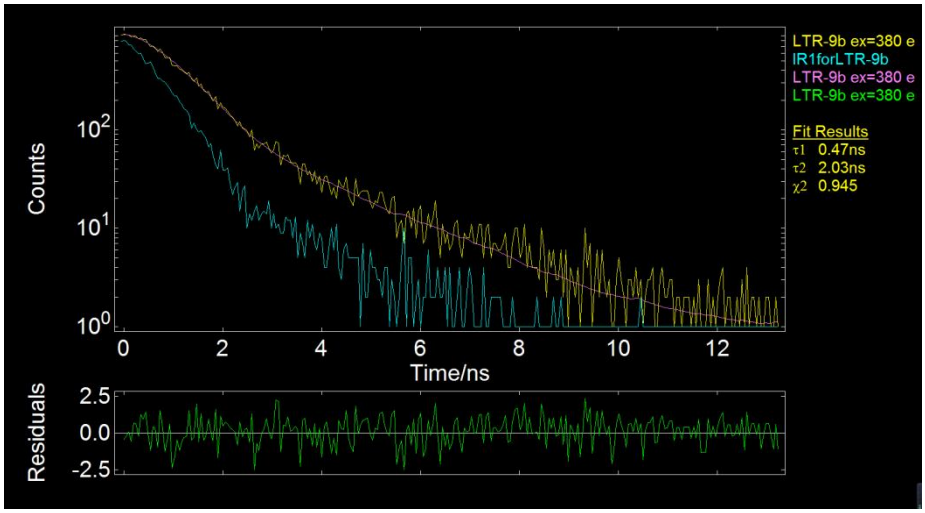

Fig. S4. PL decay curves of solid sample of **1** (λ_{ex} = 380 nm)

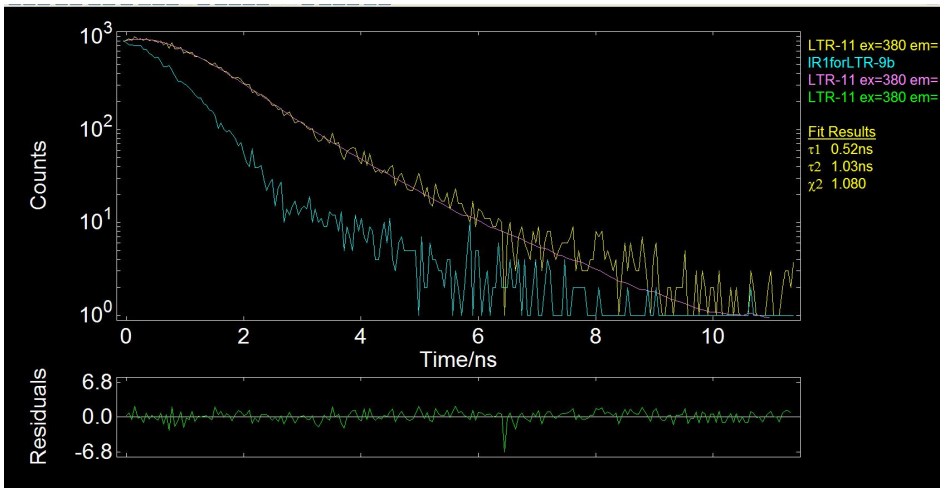

Fig. S5. PL decay curves of solid sample of **2** (λ_{ex} = 380 nm)

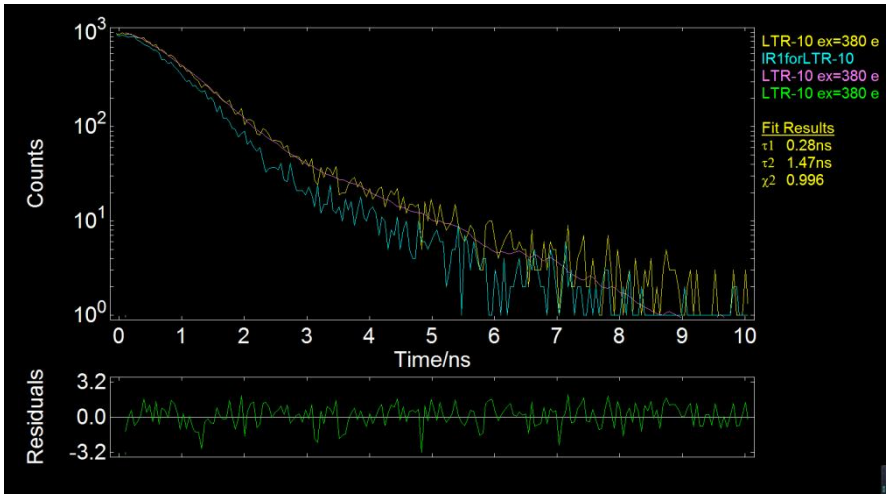

Fig. S6. PL decay curves of solid sample of **3** (λ_{ex} = 380 nm)

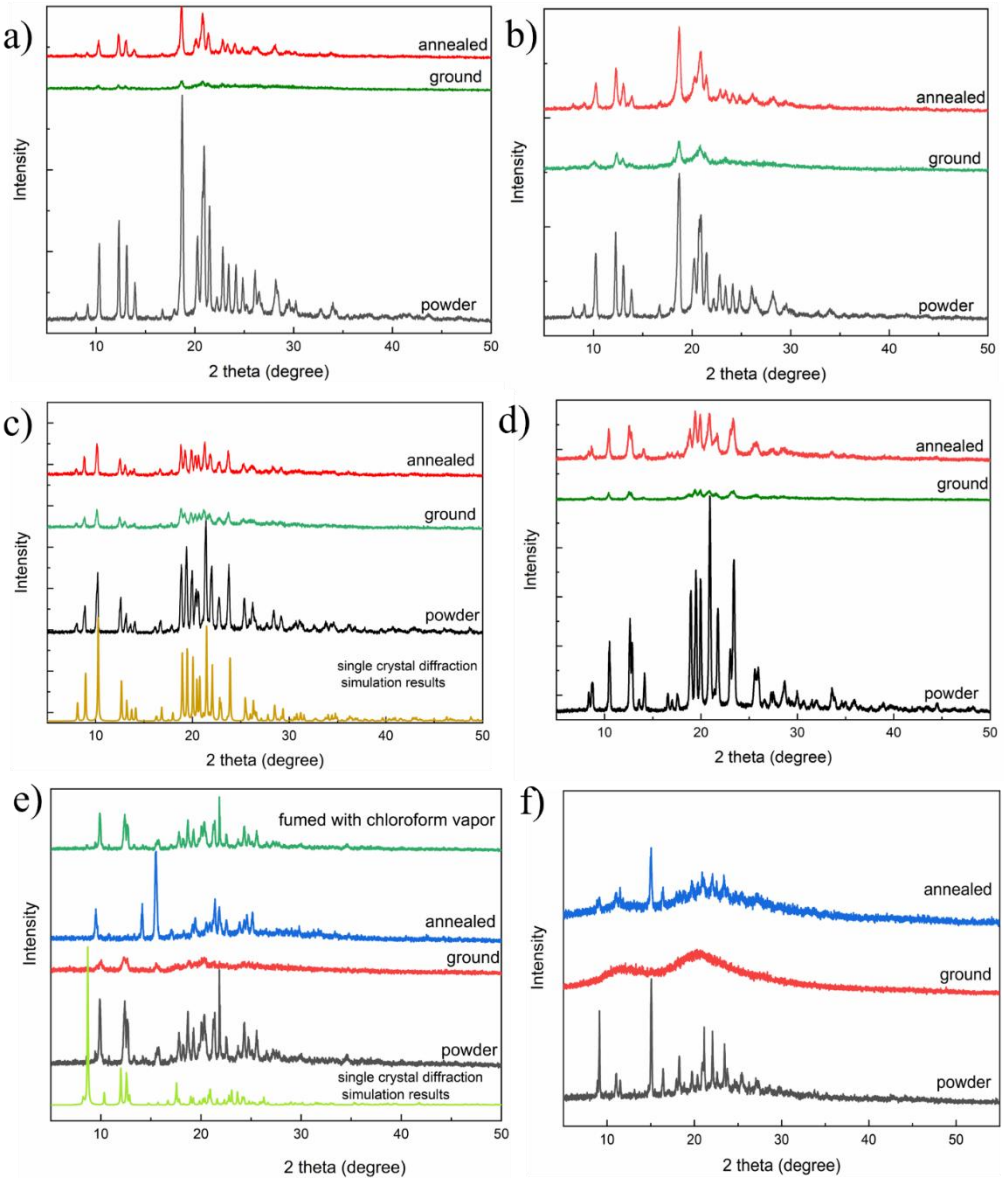

Fig. S7 PXRD patterns of a) **1**, b) **TPE-4CHO**, c) **2**, d) **TPE-3CHO** e) **3** and f) **TPE-2CHO** before and after grinding, and then annealed/fumed

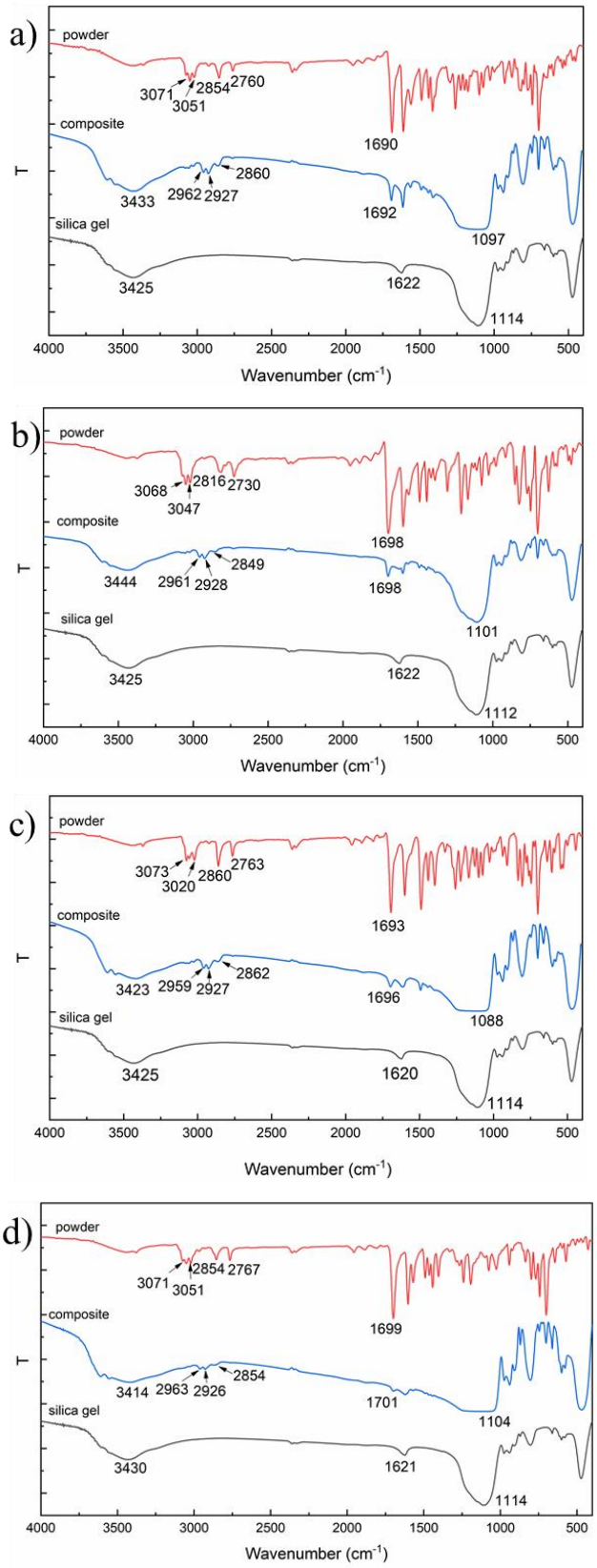

Fig. S8 FT-IR spectra of silica gel composites of a) **1**, b) **TPE-4CHO**, c) **2** and d) **3** at room temperature

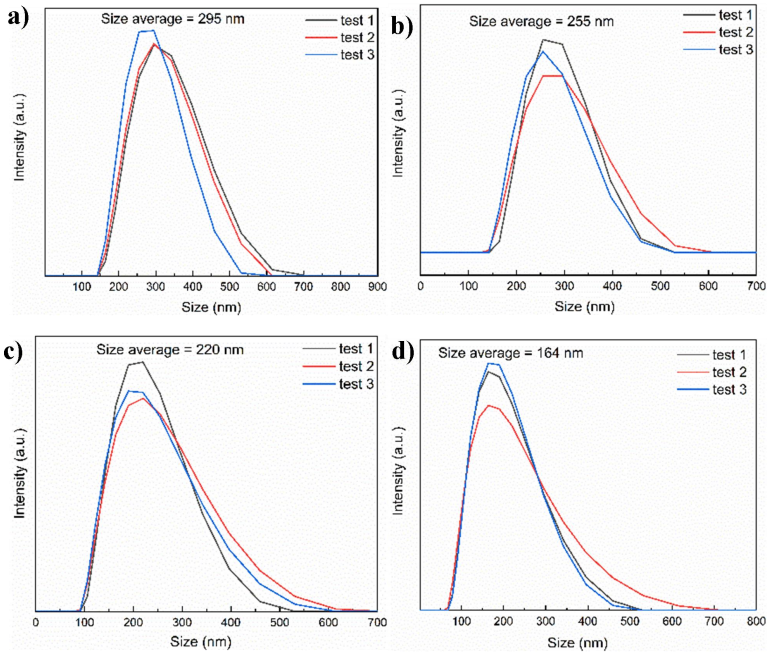

Fig. S9 DLS results of the aggregates of compound **1** with water fractions of a) 90%, b) 92%, c) 95% and d) 96%

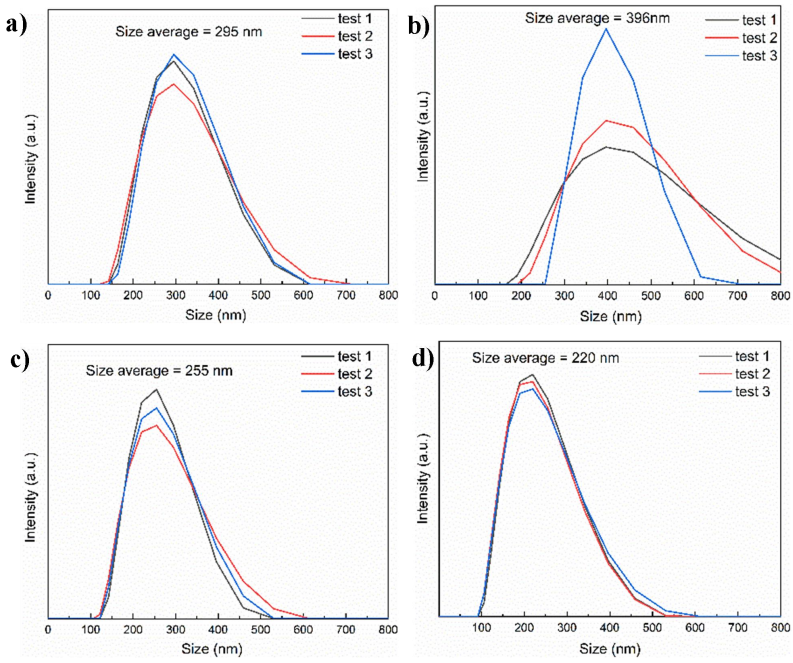

Fig. S10 DLS results of the aggregates of compound **2** with water fractions of a) 90%, b) 92%, c) 95% and d) 96%

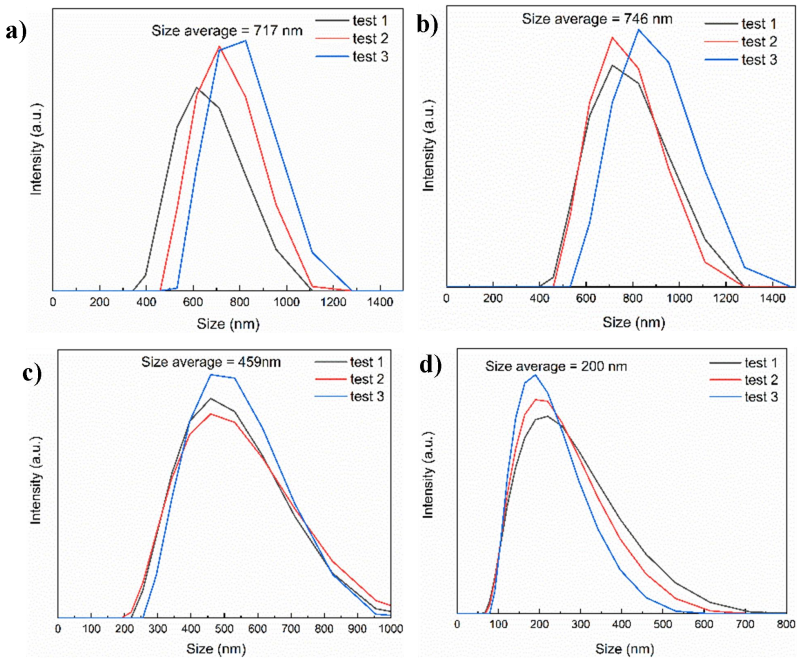

Fig. S11 DLS results of the aggregates of compound **3** with water fractions of a) 90%, b) 92%, c) 95% and d) 96%

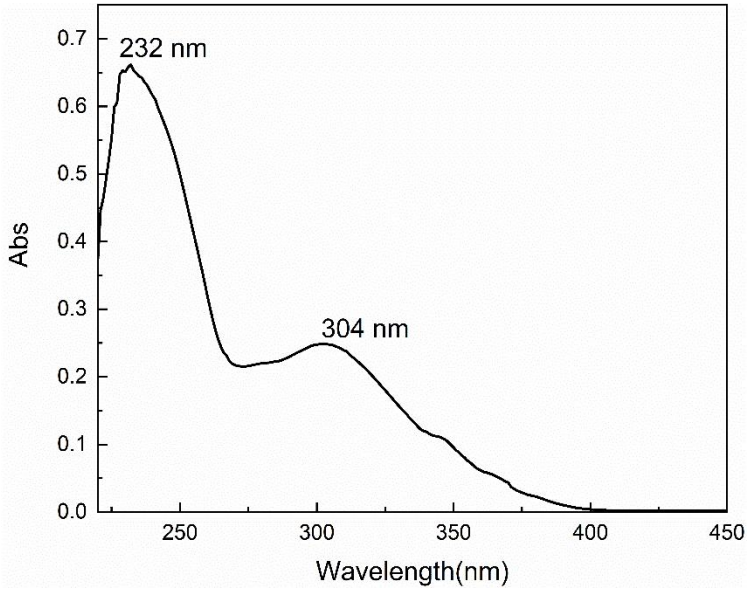

Fig. S12 Absorption spectrum of **TPE-2CHO** in THF (2×10^{-5} mol/L)

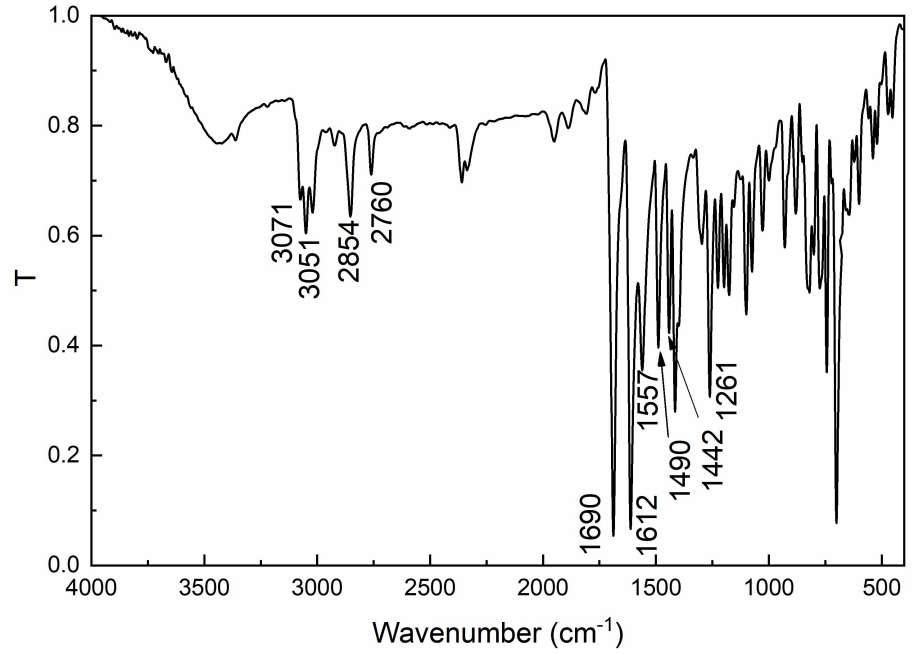

Fig. S13 FT-IR spectrum of **1** (KBr pellet)

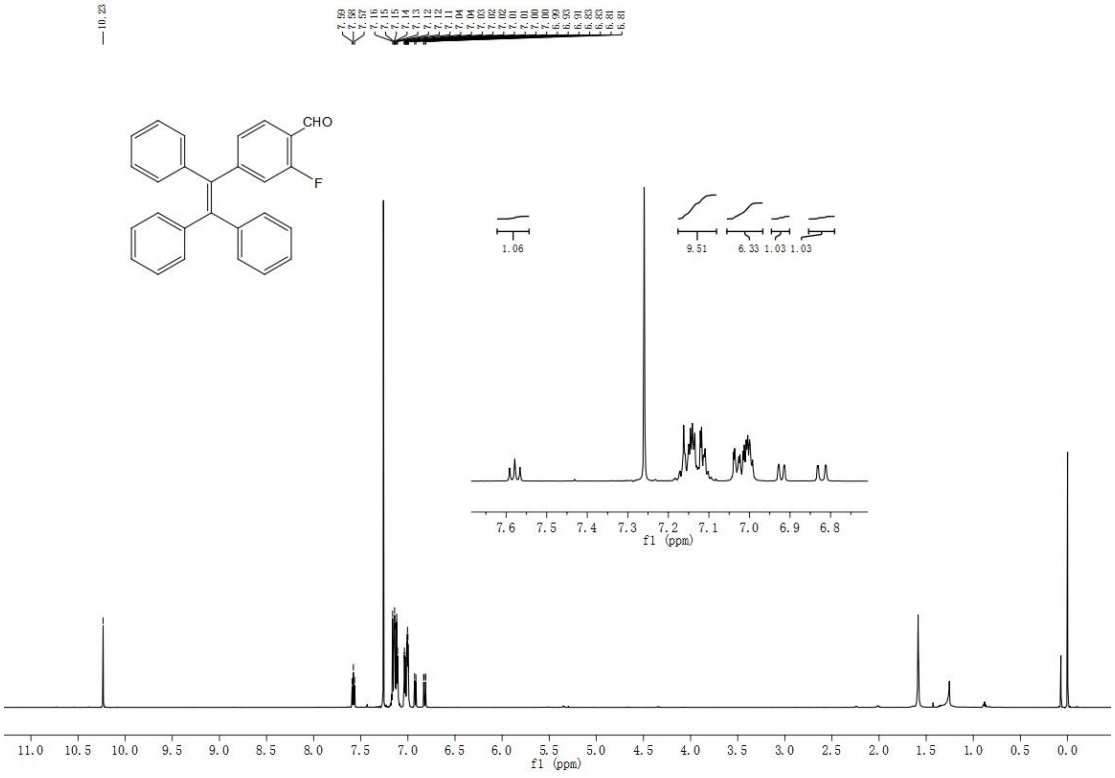

Fig. S14 ^{1}H-NMR spectrum of **1** in $CDCl_3$

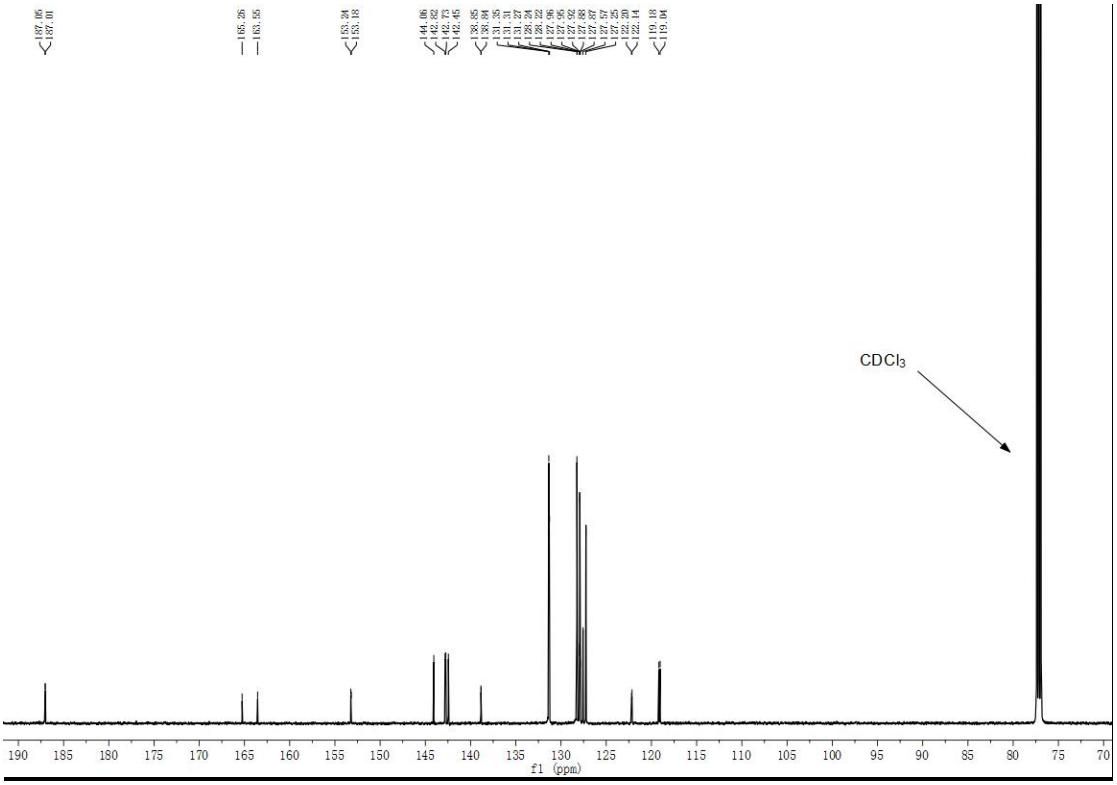

Fig. S15 ^{13}C-NMR spectrum of **1** in $CDCl_3$

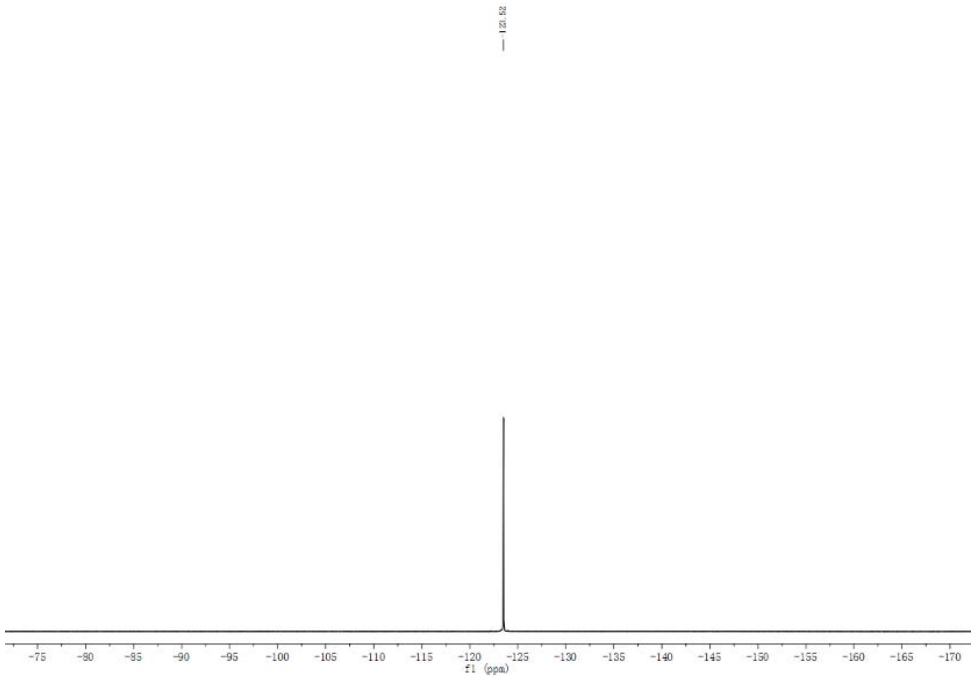

Fig. S16 ^{19}F-NMR spectrum of **1** in dichloromethane

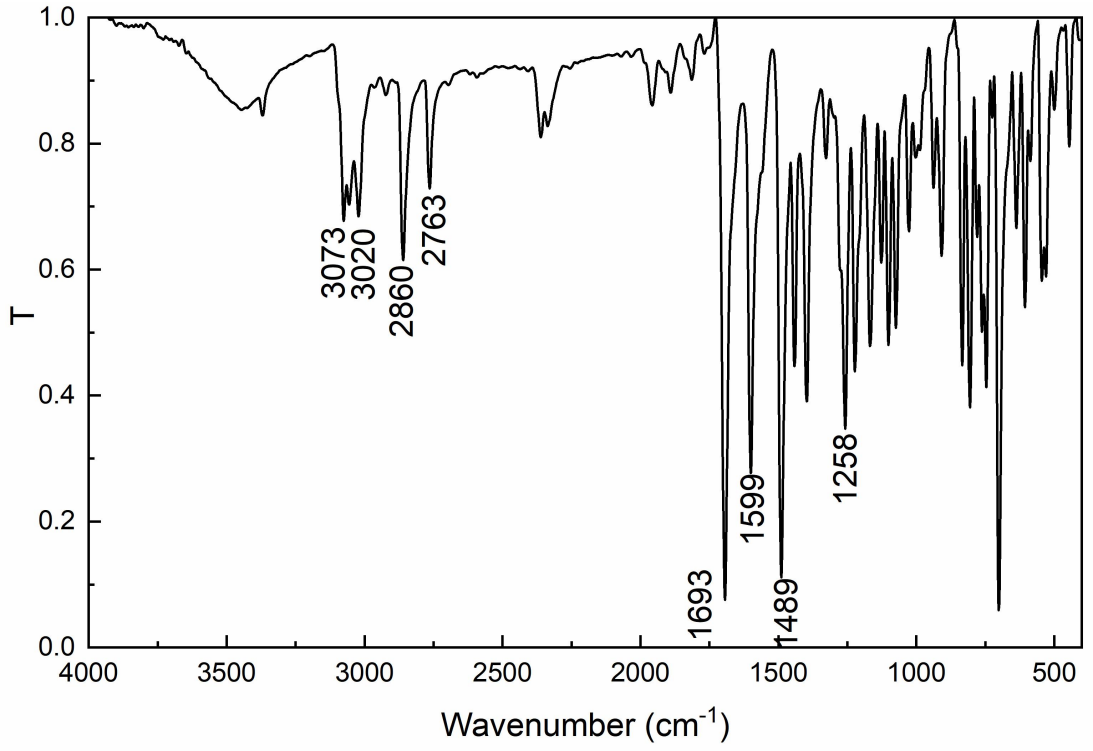

Fig. S17 FT-IR spectrum of **2** (KBr pellet)

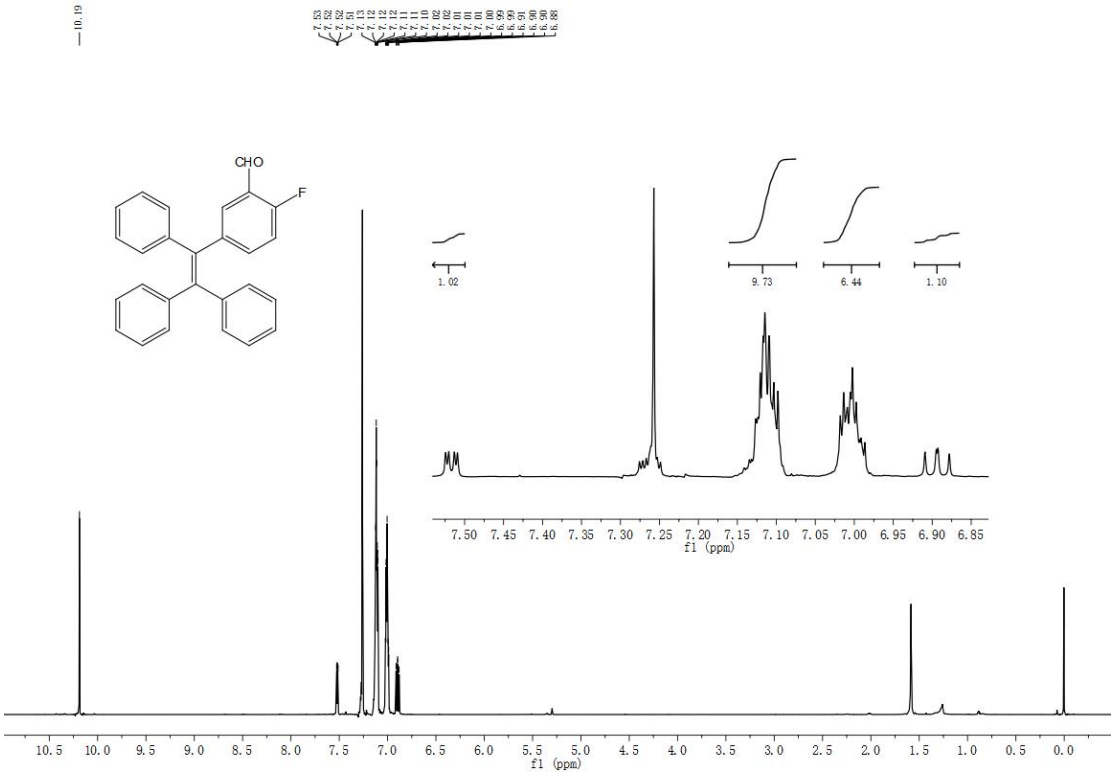

Fig. S18 ^{1}H-NMR spectrum of **2** in $CDCl_3$

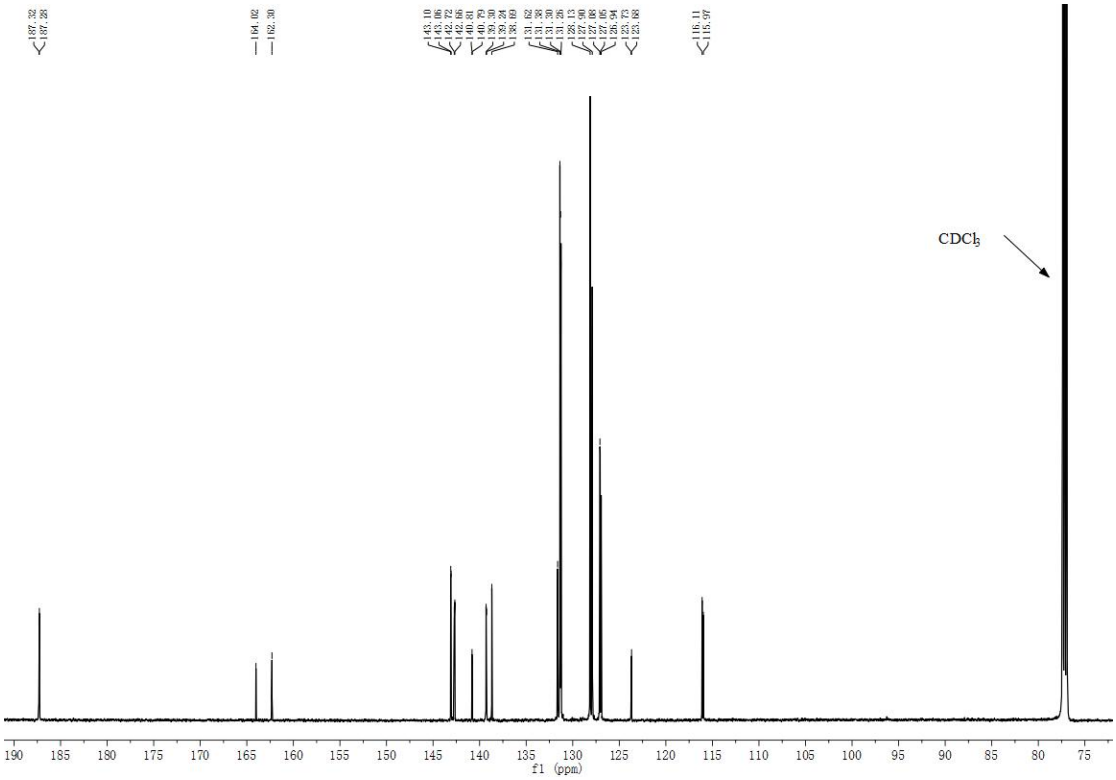

Fig. S19 ^{13}C-NMR spectrum of **2** in $CDCl_3$

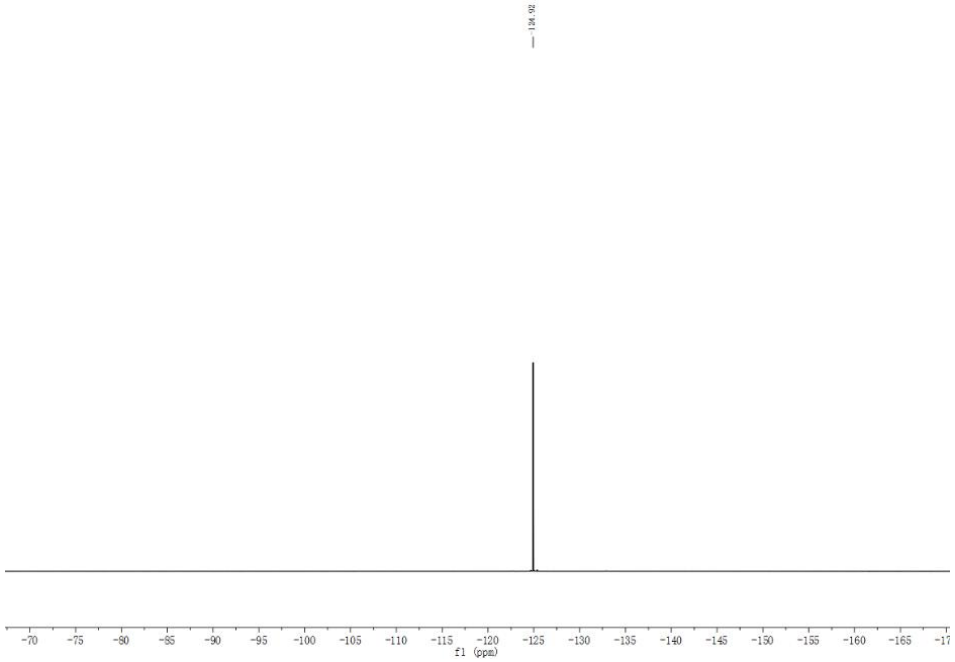

Fig. S20 ^{19}F-NMR spectrum of **2** in dichloromethane

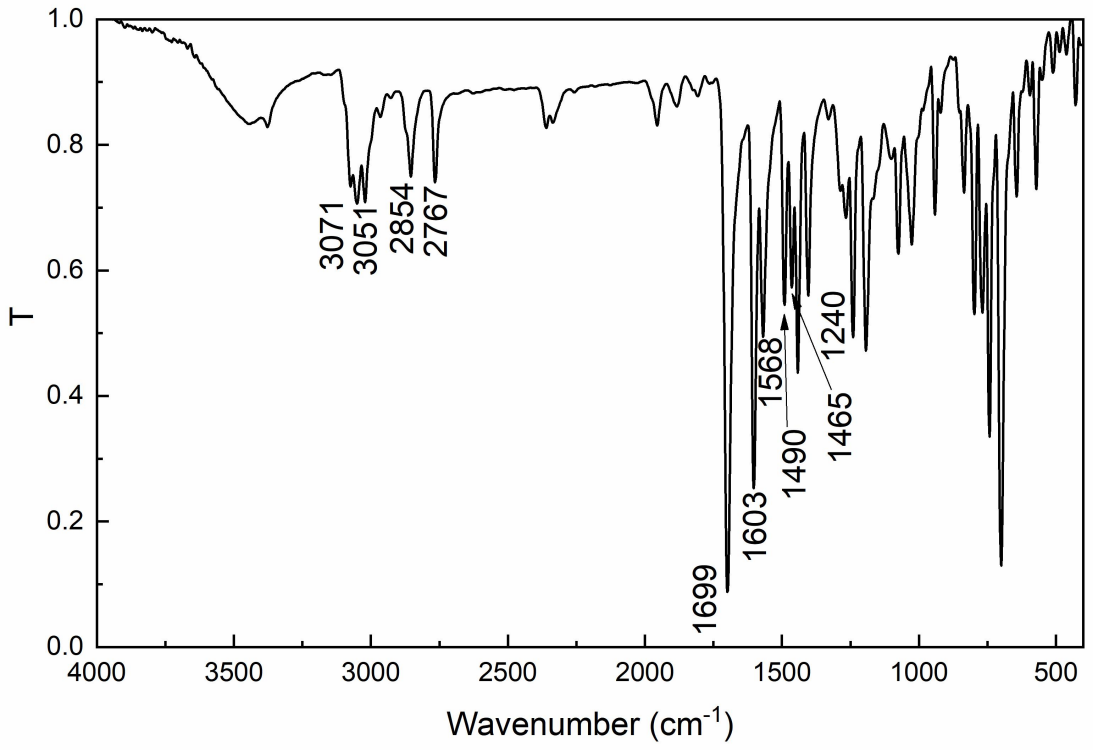

Fig. S21 FT-IR spectrum of **3** (KBr pellet)

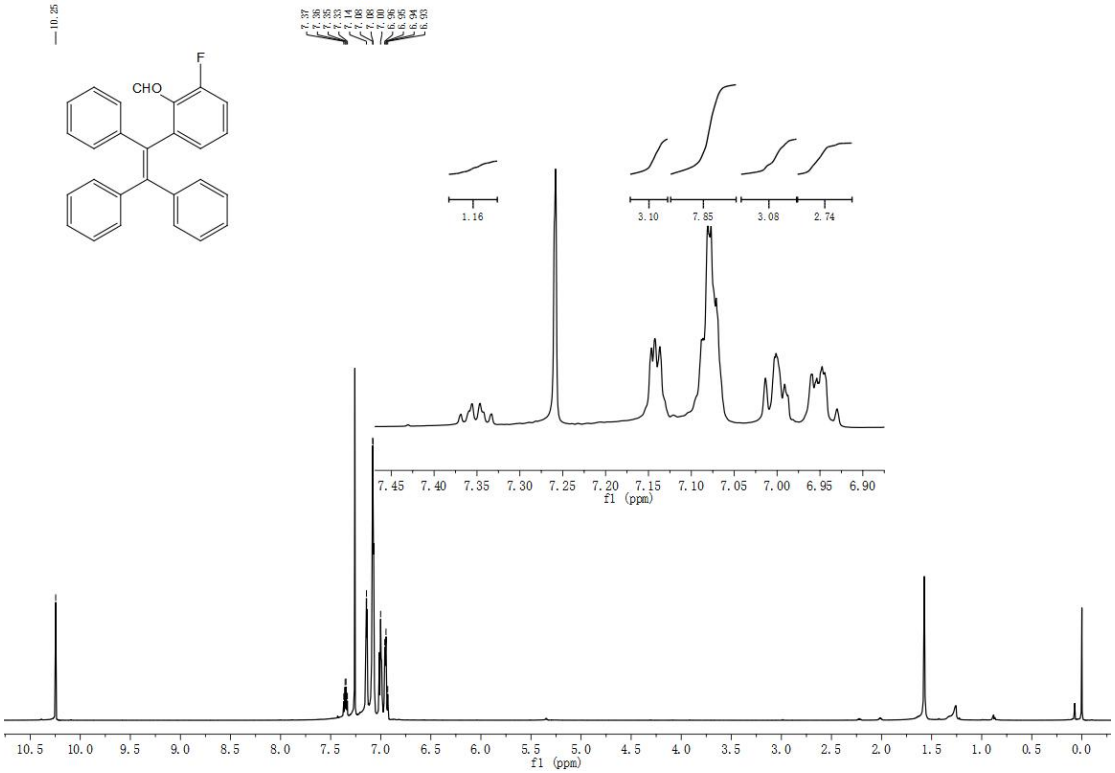

Fig. S22 ^{1}H-NMR spectrum of **3** in $CDCl_3$

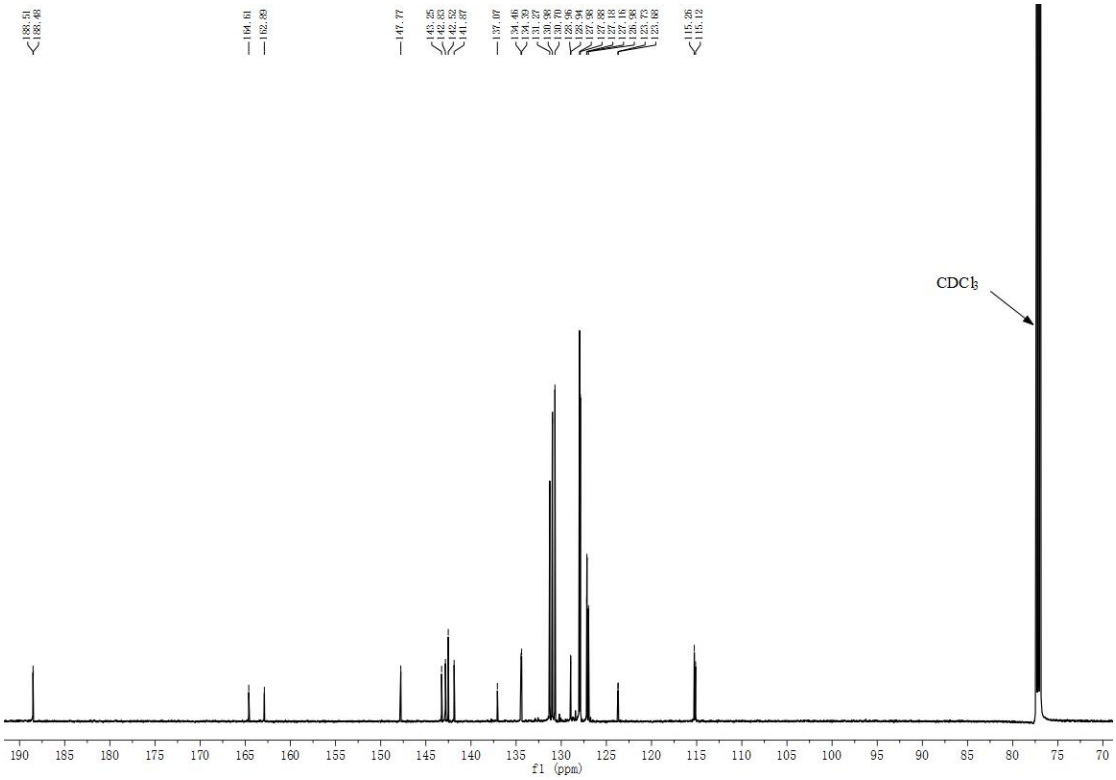

Fig. S23 ^{13}C-NMR spectrum of **3** in $CDCl_3$

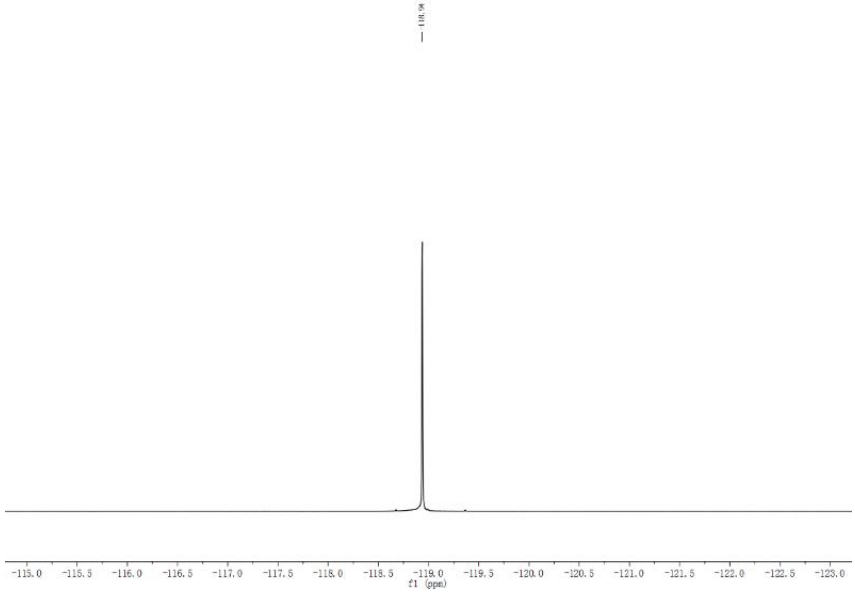

Fig. S24 ^{19}F-NMR spectrum of **3** in dichloromethane

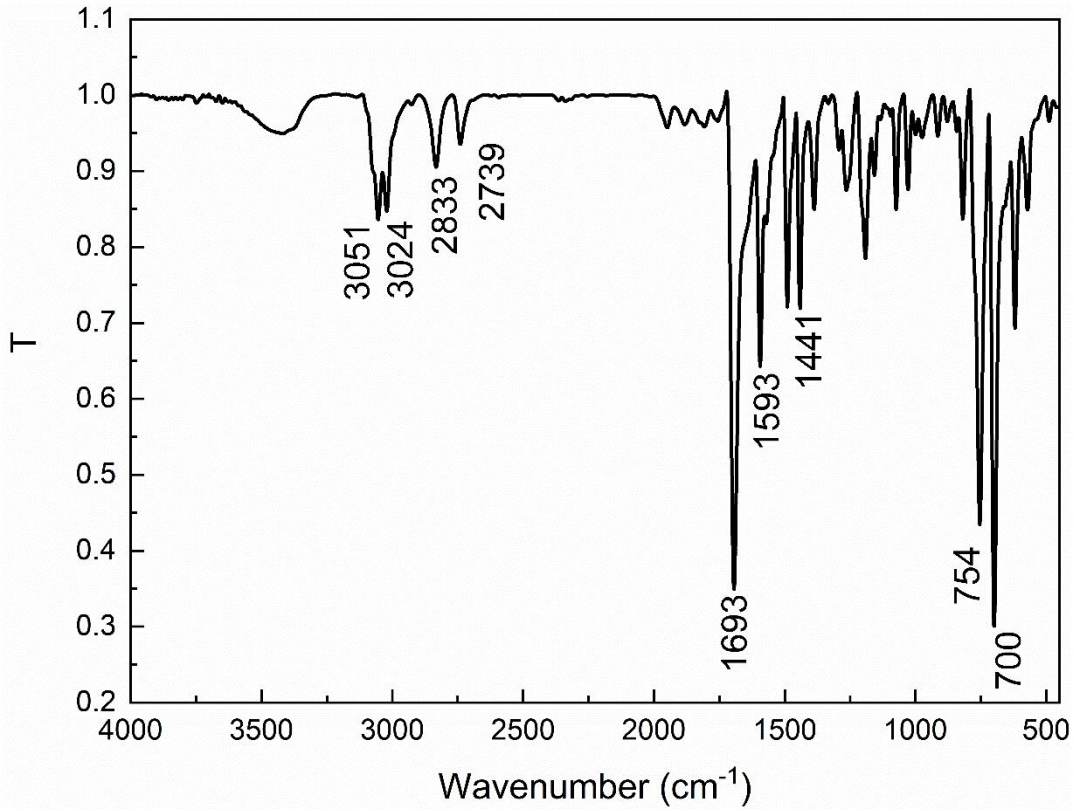

Fig. S25 FT-IR spectrum of **TPE-2CHO** (KBr pellet)

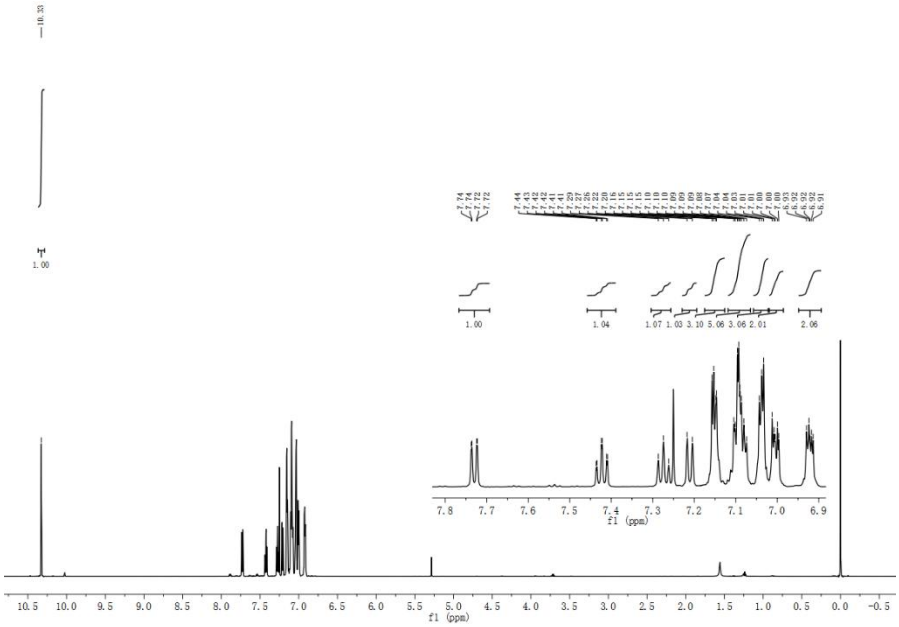

Fig. S26 ^{1}H-NMR spectrum of **TPE-2CHO** in $CDCl_3$

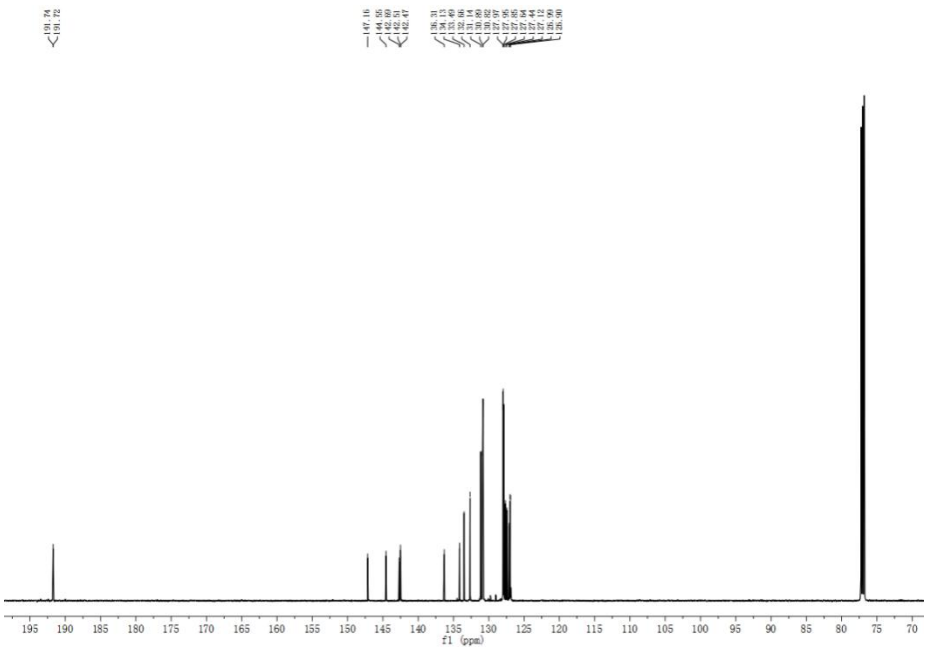

Fig. S27 ^{13}C-NMR spectrum of **TPE-2CHO** in $CDCl_3$